Achieving a Significantly Increased Efficiency in Nondoped Pure Blue Fluorescent OLED: A Quasi-Equivalent Hybridized Excited State

Shitong Zhang, Liang Yao, Qiming Peng, Weijun Li, Yuyu Pan, Ran Xiao, Yu Gao, Cheng Gu, Zhiming Wang, Ping Lu, Feng Li, Shijian Su, Bing Yang, and Yuguang Ma*

Excited state characters and components play a decisive role in photoluminescence (PL) and electroluminescence (EL) properties of organic light-emitting materials (OLEDS). Charge-transfer (CT) state is beneficial to enhance the singlet exciton utilizations in fluorescent OLEDs by an activated reverse intersystem crossing process, due to the minimized singlet and triplet energy splitting in CT excitons. However, the dominant CT component in the emissive state significantly reduces the PL efficiency in such materials. Here, the strategy is to carry out a fine excited state modulation, aiming to reach a golden combination of the high PL efficiency locally emissive (LE) component and the high exciton utilizing CT component in one excited state. As a result, a quasi-equivalent hybridization of LE and CT components is obtained in the emissive state upon the addition of only an extra phenyl ring in the newly synthesized material 4-[2-(4′-diphenylamino-biphenyl-4-yl)-phenanthro[9,10-d]imidazol-1-yl]-benzonitrile (TBPMCN), and the nondoped OLED of TBPMCN exhibited a record-setting performance: a pure blue emission with a Commission Internationale de L'Eclairage coordinate of (0.16, 0.16), a high external quantum efficiency of 7.8%, and a high yield of singlet exciton of 97% without delayed fluorescence phenomenon. The excited state modulation could be a practical way to design low-cost, high-efficiency fluorescent OLED materials.

1. Introduction

Nowadays, the organic light-emitting diodes (OLEDs)[1] are playing a significant role in the new generation of flat-panel display and solid-state lighting due to their advantages.[2–7] Different from the inorganic light-emitting diodes, the recombination of the injected holes and electrons form strongly bound excitons that exhibit distinct spin state in OLEDs: singlet and triplet in a ratio of 1:3 according to the spin statistics rules. Thus, the fluorescent materials generally suffer from an upperlimit of exciton utilizing efficiency (η_s) to 25% in OLEDs, because only singlet excitons are spin allowed for radiative decay to ground state. The η_s can be increased to nearly 100% by employing phosphorescent materials due to heavy atom effect to greatly enhance the intersystem crossing (ISC).[2–4] However, there are still some issues to be considered. For instance, the high cost of OLEDs commercialization due to the use of expensive metals, the insufficiency to full-color display, especially the lack of blue phosphorescent materials, and so on. To address these issues, scientists recently focused their attentions back on the fluorescent materials, aiming at developing high triplet exciton utilization, low-cost OLEDs based on metal-free fluorescent materials. Two promising approaches have been proposed for triplet exciton utilization: triplet–triplet annihilation (TTA) and thermally activated delayed-fluorescence (TADF). TTA process could provide a theoretically maximized exciton utilization of 62.5%, in which one extra singlet exciton will be generated by the fusion of two triplet excitons.[5,14] In contrast, TADF process is more effective than TTA: a nearly 100% exciton utilization could be harvested by means of thermal energy-assisted reverse intersystem crossing (RISC) process from T_1 to S_1 state.[6] These two kinds of delayed-fluorescence methods do dramatically improve the overall electroluminescence (EL) efficiency, nevertheless, like the phosphorescence OLEDs, their efficiencies usually suffer from serious rolling-off at high current density that originates from the inevitable concentration accumulation due to the long lifetime of T_1 excitons. Therefore, they are usually applied in the

S. Zhang, L. Yao, Q. Peng, Dr. W. Li, Y. Pan, R. Xiao, Y. Gao, Dr. C. Gu, Prof. P. Lu, Prof. F. Li, Prof. B. Yang
State Key Laboratory of Supramolecular Structure and Materials
Jilin University
Changchun 130012, P.R. China
E-mail: yangbing@jlu.edu.cn

S. Zhang, L. Yao, Y. Pan, Y. Gao, Prof. B. Yang
College of Chemistry
Jilin University
Changchun 130012, P.R. China

Prof. Z. Wang
School of Petrochemical Engineering
Shenyang University of Technology
Liaoyang 111003, P.R. China

Prof. S. Su, Prof. Y. Ma
State Key Laboratory of Luminescent Materials and Devices
South China University of Technology
Guangzhou 510640, P.R. China

DOI: 10.1002/adfm.201404260

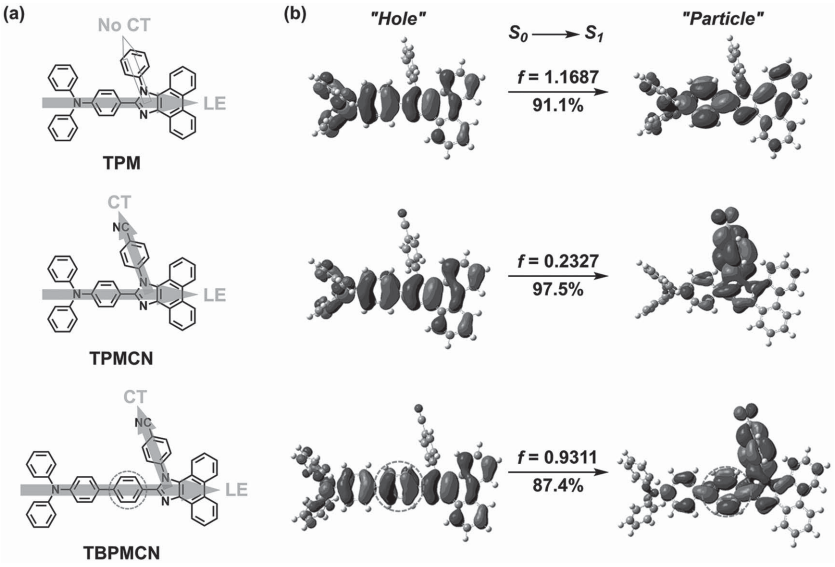

Figure 1. a) Chemical structures and b) the $S_0 \rightarrow S_1$ NTO of TPM, TPMCN, and TBPMCN. Herein, *f* represents the oscillator strength, and the weights of hole–particle are given for the $S_0 \rightarrow S_1$ excitations. The data of TPM and TPMCN are taken from the literature[7d] for comparison to TBPMCN as mentioned in the main text.

doped OLEDs for high EL efficiency, which is against the easy fabrication of device in comparison with the nondoped OLEDs.

We recently established a series of nondelayed fluorescent materials that also breaks through the 25% upper limit of η_s in OLEDs. Their excited states are featured as hybridized local and charge-transfer (HLCT) state, that is, a special excited state with obviously coexisted locally emissive (LE) and charge-transfer (CT) character components.[7] The LE component provides a high radiative transition rate that is related to a high photoluminescence (PL) efficiency (η_{PL}), whereas the CT component is responsible for a sufficiently small singlet–triplet energy splitting (ΔE_{ST}), as a result of the nearly disappeared electron exchange interaction with an increased spatial separation between electron and hole wavefunctions in CT-like excitons, which enables a high η_s arising from the enhanced RISC (T→S) process along high-lying excited states.[7b,7e,8] Therefore, in principle, such excited state property could harvest the maximized EL efficiency from a compatible coexistence between high η_{PL} and high η_s, corresponding to a golden combination between LE component and CT component. What is more, the T_1 concentration quenching problem could be hopefully suppressed to a lower degree due to the restricted delayed fluorescence, if the triplet CT states were located on the high-lying triplet energy levels, which is of shorter lifetimes than the T_1 state. Thus, it is possible to realize the highly efficient nondoped OLED by using HLCT materials. 4-(2-(4-(Diphenylamino) phenyl)-1H-phenanthro[9,10-d]imidazol-1-yl) benzonitrile (TPMCN, **Figure 1**) is such an example. With the HLCT character in its excited state, it can harvest an exceeding η_s of 85% in nondoped EL device.[7d] As mentioned above, this high η_s in TPMCN can be ascribed to the incorporation of CT characters in the emissive state as a result of the substitution of cyano group. As a comparison, the cyano-free LE material TPM (Figure 1) only possesses a very low η_s of 16%. Despite the fact that the dominated CT component in TPMCN leads to a serious decrease of η_{PL} from 35% to 13% in the film state, the EL efficiency of TPMCN is still twice as high as that of TPM under the same device structures. This achievement is ascribed to the fact that the enhancement of η_s is far superior to the sacrifice of η_{PL}. For the purpose of the maximization of the EL efficiency, a further fine modulation in the HLCT state is confidentially necessary, in order to achieve balanced LE and CT components in the excited state, or to strengthen the LE component while maintaining the present CT component. This work focuses on a redesigned new material 4-[2-(4′-diphenylaminobiphenyl-4-yl)-phenanthro[9,10-d]imidazol-1-yl]-benzonitrile (TBPMCN, Figure 1) based on TPMCN, and the better understanding on the relationship between excited state properties and EL performances upon the excited state modulation.

2. Results and Discussions

2.1. Molecular Design

2.1.1. Calculated Excited State Properties

The synthesis route of TBPMCN is outlined in **Scheme 1**. TBPMCN inherits the orthogonal donor and

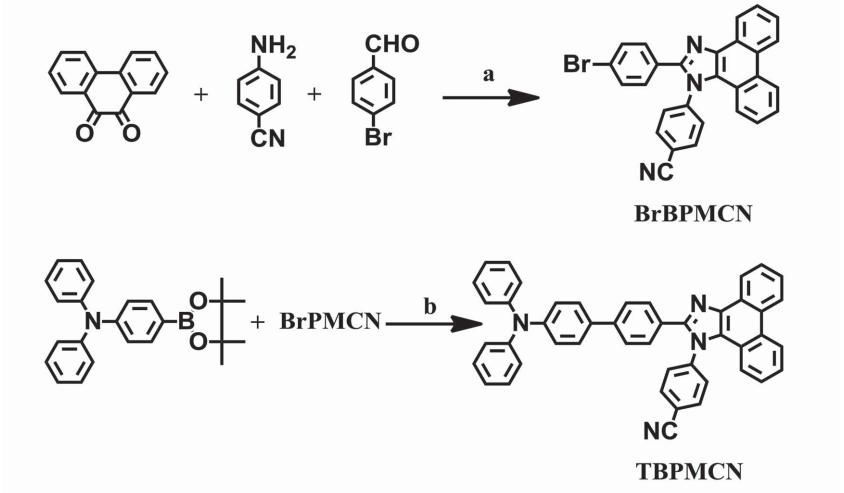

a= CH_3COOH: CH_3COONH_4, 120℃, 2h; b= Toluene: $Pd(Pph_3)_4/K_2CO_3$ aq, 90℃, ~2d

Scheme 1. Synthesis route of TBPMCN.

acceptor architecture feature of TPMCN. In Figure 1, the triphenylamine-benzolyl-phenatheroimmidazole (TBPM) backbone acts as the electron donor and the orthogonal benzonitrile serves as the acceptor. From TPMCN to TBPMCN, an additional phenyl ring is inserted between triphenylamine and phenathero-imidazole with the extended π-conjugation to increase LE component, for the purpose of the improvement of η_{PL} and simultaneously maintain the strength of donor and acceptor (or the CT component) to the best extent. In the first step, density functional theory (DFT/M06-2X/6-31G**) calculations combined with the natural transition orbital (NTO)[9] analysis are used to describe the excited-state properties of the two materials (Figure 1). For the S_1 state, NTO "hole" and "particle" of TBPMCN are obviously similar to those of TPMCN. For both the two molecules, "holes" are delocalized over the whole horizontal backbone, while "particles" are mainly localized on the vertical benzonitrile and other several fragments: phenatheroimidazol and the adjacent biphenyl or phenyl rings. As a comparison, a similar CT transition character is maintained from the horizontal backbone to the vertical benzonitrile in the S_1 state of both TBPMCN and TPMCN, whereas the overlap density between "hole" and "particle" is significantly expanded due to the insertion of an extra phenyl ring in TBPMCN, indicating an enhanced LE component in S_1 state relative to that of TPMCN. For this special S_1 state of TBPMCN, the oscillator strength is calculated to be 0.9311, which is fourfold as high as that of TPMCN (0.2327), implying that a much higher η_{PL} could be expected in TBPMCN than in TPMCN, as a result of an additional phenyl ring that totally contributes to the increased LE component in S_1 state.

2.1.2. Quasi-Equivalent Hybridization in TBPMCN

To our interest, the NTO of S_2 and S_1 excited states in both TBPMCN and TPMCN exhibit a hybrid-splitting state character that derives from the interstate coupling between LE (TPM→TPM or TBPM→TBPM) and CT (TPM→benzonitrile or TBPM→benzonitrile) states (Figure S4, Supporting Information). It is noteworthy that the orbital symmetry of the "particle" on the benzonitrile group of the two molecules are exactly in the opposite phase between S_1 and S_2 states, indicating that the interstate coupling occurs through the positive and negative linear combination between horizontal LE and vertical CT, respectively, as shown in Equation (1)

$$\psi_{S1/S2} = \lambda_{LE} \cdot \psi_{LE} \pm \lambda_{CT} \cdot \psi_{CT} \quad (1)$$

Thus, both S_1 and S_2 states should be considered as a hybrid state caused by the cyano substitution in TBPMCN and TPMCN.[10] On the other hand, some other slight differences of hybrid states can also be found between TBPMCN and TPMCN. In the case of TBPMCN, the S_1 and S_2 excited states are very similar in energy, oscillator strength (Table S3, Supporting Information), and the corresponding NTO distribution, which indicate a quasi-equivalent hybridization between LE and CT states due to their almost isoenergetic initial states. As a contrast, for TPMCN, the S_1 and S_2 excited states demonstrate a quite significant difference in energy, oscillator strength, and NTO image, which is caused by the nonequivalent hybridization between LE and CT initial states (Figure S4, Supporting Information). Compared with the nonequivalent hybridization, the quasi-equivalent hybridization is expected to achieve the golden combination between high η_{PL} and high η_s, and further to maximize the EL efficiency in the OLED, due to the more balanced LE and CT components in HLCT state of TBPMCN than that of TPMCN.

2.2. Photophysical Properties

2.2.1. Ultraviolet–Visible (UV–Vis) Absorption and PL Properties

The excited state properties of these two materials are further examined by characterizing their detailed photophysical properties. The UV–PL spectra of these two compounds are illustrated in **Figure 2**a. Although the two materials exhibited almost the same absorption peak location, the absorption peak of TBPMCN is obviously narrower than that of TPMCN, revealing to a more π–π^* like character. For the PL spectra, apart from the same narrower trend as that in the UV spectra, the PL peak of TBPMCN gives an unexpected 25 nm blue-shift comparing to TPMCN, which is completely opposite to the common sense that the extension of π-conjugation generally leads to a red shift in PL spectra.[11] In essence, this "abnormal" blue-shift can be predominantly attributed to the enhanced LE component that is equivalent to the more suppressed CT component in the emissive state of TBPMCN. As a matter of fact, the competition of two mechanisms results in the blue shift in PL spectra from TPMCN to TBPMCN. Specifically, the extension of LE component leads to the red shift of PL spectrum, meanwhile the suppressed CT component results in the blue shift of PL spectrum, upon the insertion of an additional phenyl ring. As for the result, the latter factor is more dominant than the former one. Actually, a certain overlap (some self-absorption) can be found between UV and PL spectra of TBPMCN, which is revealed to a more LE-like character from the expanded conjugation along horizontal backbone in TBPMCN than in TPMCN. In contrast, the η_{PL} (vs quinine sulphate) of the non-self-absorption molecule TPMCN in THF is merely 7.8%, assigned to the intrinsic property that the CT state always causes an extremely low PL efficiency.[11] Nevertheless, the η_{PL} of TBPMCN in THF is as high as 79%, reflecting an obvious LE state emission character. The same trend can also be found in solid film state. The PL peaks of TPMCN and TBPMCN are located at 460 and 445 nm, respectively, and the η_{PL} for TPMCN and TBPMCN are measured as 13% and 40%, respectively, proving that TBPMCN is surely more efficient as we desired. What is more, the large blue shift relative to TPMCN makes TBPMCN more attractive as a potential pure blue OLED emitter.

2.2.2. Solvatochromic Effects

Both the two materials demonstrate obvious solvatochromic shifts with the increase of solvent polarity, indicating that the emissive states of these two materials are of typical CT characters (Figure 2b, **Table 1**).[12] The solvatochromic shift

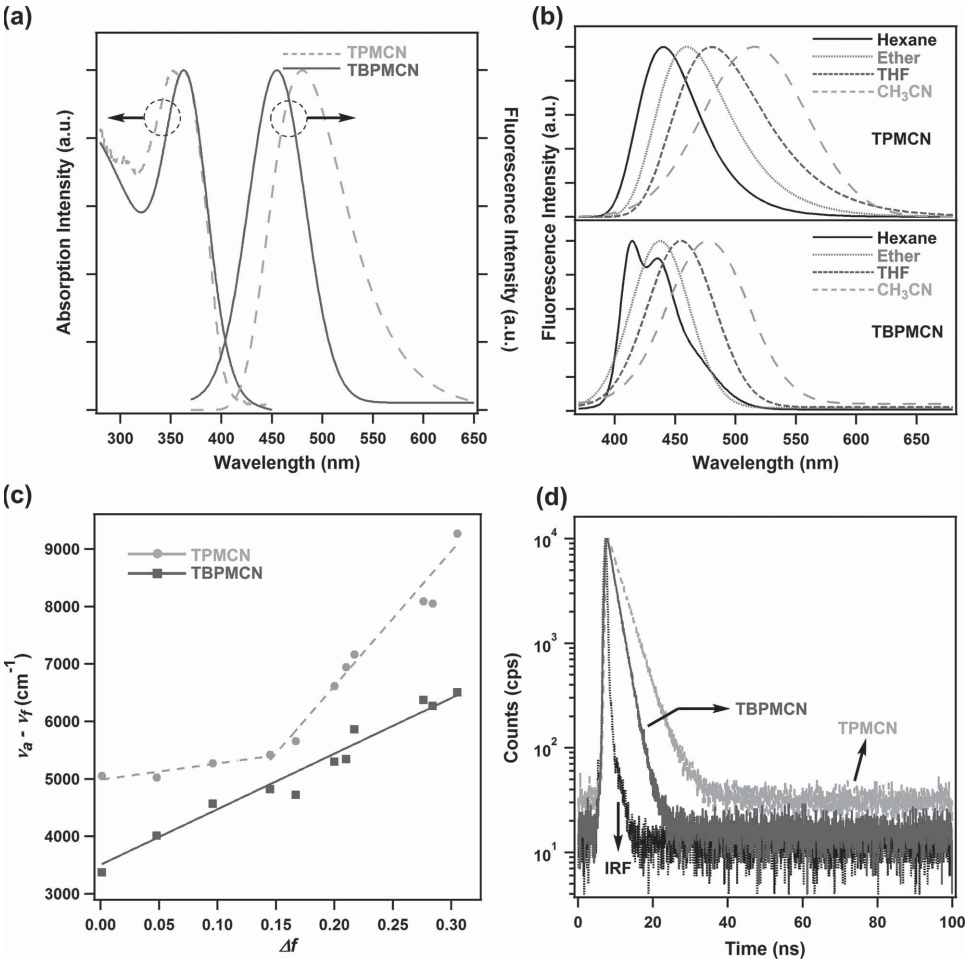

Figure 2. Comparisons on photophysical properties of TPMCN and TBPMCN. a) UV–PL spectra in tetrahydrofuran (THF) of TPMCN and TBPMCN. b) Solvatochromic PL spectra of TPMCN and TBPMCN. c) Solvatochromic Lippert–Mataga models of TPMCN and TBPMCN. The solid squares represent the Stokes' shift in different solvents, the lines are the correlated solvatochromic models of the two materials, respectively. The solvents and other photophysical properties such as Stokes' shifts and ηPL-s are listed in the Supporting Information, see Section SI-1. d) Transient PL spectra in THF of TPMCN and TBPMCN. The concentrations of the solutions are controlled to less than 1×10^{-5} mol L^{-1} to guarantee that the solutions are diluted solutions. The data of TPMCN are taken from a previous study.[7d]

of TBPMCN (55 nm) is much smaller than that of TPMCN (78 nm) from hexane to acetonitrile. Especially, in hexane, TBPMCN exactly demonstrates a LE-like character because of the existence of the vibrational fine structure in PL spectrum. Compared to the broad and smooth PL spectrum of TPMCN, the LE character of the S_1 state in TBPMCN should be much stronger than that in TPMCN. In different solvents, the full width at half maximum (FWHM) of TBPMCN is narrower than that of TPMCN, and TBPMCN possesses higher PL efficiency, as a result of the enhanced LE component in the emissive state.

Table 1. Photophysical properties of TPMCN and TBPMCN in different solvents.

		TPMCN						TBPMCN					
Solvents	Δf	ν_a[a] [nm]	ν_f[a] [nm]	ν_a-ν_f[b] [cm^{-1}]	FWHM[c] [nm]	η_{PL}[d] [%]	Lifetime[e] [ns]	ν_a[a] [nm]	ν_f[a] [nm]	ν_a-ν_f[b] [cm^{-1}]	FWHM[c] [nm]	η_{PL}[d] [%]	Lifetime[e] [ns]
Hexane	0.0012	360	440	5051	61	26	3.05	364	415	3376	53	≈100	1.14
Ether	0.167	365	460	5658	73	13	3.22	363	440	4821	57	94	1.51
THF	0.21	360	480	6944	88	7.8	3.52	364	451	5300	65	79	1.83
Acetonitrile	0.305	350	518	9266	101	0.81	3.98	363	470	6272	82	24	2.12

[a] ν_a and ν_f are the UV and PL peaks in different solvents, respectively; [b] Stokes shift in different solvents; [c] The full width at half maximum; [d] Measured versus quinine sulphate; [e] Measured at the peak wavelengths in different solvents.

We further consider the solvatochromic effect using Lippert–Mataga model, in which the *X*-axis represents the solvent polarity factor *f*, and the *Y*-axis stands for the Stokes' shift (Figure 2c, Section SI-1, Supporting Information).[12] The dipole moment of S_1 exciton can be estimated by the slope of the fitted line of experimental points. Notably, different from the two-section line of TPMCN, TBPMCN exhibits only one slope of 9667 (r = 0.98), corresponding to one excited state dipole moment of 17 D. This dipole moment is slightly smaller than that of the CT section in TPMCN (≈21 D, r = 0.97), but much larger than the LE section (≈8 D, r = 0.97).[7d] In the case of TPMCN, the two-section line corresponds to the two different exciton states with two distinguishable small and large dipole moments in low-polarity solvents and high-polarity solvents, respectively. This is a strong evidence that the nonequivalent hybridization occurs between LE and CT initial states in TPMCN (Figure S4, Supporting Information), which forms LE-based HLCT state in low-polarity solvents and CT-dominated HLCT state in high-polarity solvents, respectively. Consequently, in low-polarity solvents, the S_1 exciton behaves like the LE-like excitons with small dipole moment (≈8 D), while the S_1 exciton becomes CT-like excitons with large dipole moment (≈21 D) in high-polarity solvents, as a result of the more sensitive CT state (78 nm solvatochromic red-shift from hexane to acetonitrile) in TPMCN than that in TBPMCN (55 nm solvatochromic red-shift).[13] However, TBPMCN seems not to obey the same rule. In TBPMCN, the dipole moments in both low- and high-polarity solvents are undistinguishable. Actually, even in very-low-polarity solvent such as hexane, the good linearity still retains, which means that the large excited-state dipole moment remains unchanged regardless of the solvent polarity. This undistinguishable large dipole moment in all solvents well supports the sufficiently hybridized LE and CT components due to the stronger interstate coupling between LE and CT states in TBPMCN, corresponding to a quasi-equivalent hybridization between LE and CT states (Figure S4, Supporting Information). As a benefit of quasi-equivalent hybridization, even in the high-polarity solvent such as acetonitrile, TBPMCN still remains a relatively high η_{PL} of 24%, which is very close to the highest value of η_{PL} in TPMCN among all solvents (26%). The differences on the hybridization extents between TPMCN and TBPMCN can also be easily understood by the discussions on the energy diagrams and the NTO distributions (Figure S4, Supporting Information). In addition, the Lippert–Mataga model could also provide a set of "dynamic" messages with the change of emissive state properties in different solvents. For TPMCN, the nonequivalent hybridization state with more CT-like character not only causes relatively low PL efficiencies in all solvents, but also makes it more sensitive to the solvent polarities. That is the reason why TPMCN demonstrates totally different excited state character in low- and high-polarity solvents. In contrast, the quasi-equivalent hybridization state of TBPMCN exhibits more stable composition and property upon the solvent polarizations than TPMCN. That is to say, it is convinced that the emissive state of TBPMCN behaves a sufficiently hybridized LE and CT character with the balanced LE and CT components as we expected.

2.2.3. Time-Resolved Photoluminescence and S_1–T_1 Energy Gap

It is noticeable that both TPMCN and TBPMCN do not possess delayed lifetime component (only prompt species for TPMCN (3.52 ns) and TBPMCN (1.83 ns), Figure 2d), indicating that these two materials are essentially different from the TADF materials in luminous mechanism. We then carried out the time-resolved PL measurement under 77 K to observe the PL characters of these two materials in different time scales, and to evaluate their S_1–T_1 energy gaps. On one hand, the delayed PL spectra in different time scales of these two materials are all phosphorescence instead of TADF (**Figure 3**b), or they would be just the same as the nondelayed fluorescent ones in Figure 3a. On the other hand, the energy gap between S_1 and T_1 of TBPMCN can be estimated as ≈570 meV from Figure 3a, which is even larger than that of TPMCN (≈295 meV) at 77 K. This large energy gap is almost impossible for the RISC process along the $T_1 \rightarrow S_1$ channel like typical TADF materials. As a result, in the temperature-dependent PL measurement (Figures S2 and S3, Supporting Information), TBPMCN shows almost no obvious PL enhancement with the temperature increases from 80 to 380 K, and also no long-lifetime PL component in the transient PL spectra.

2.3. EL Performances

The nondoped EL device was then fabricated to investigate the intrinsic relationship between excited state properties and its EL performance in TBPMCN. The typical device structure was prepared with the configuration of ITO/PEDOT:PSS (40 nm)/NPB (80 nm)/TCTA (5 nm)/TBPMCN (20 nm)/TPBi (40 nm)/LiF (1 nm)/Al(120 nm). The device exhibited a pure blue EL emission with the Commission Internationale de L'Eclairage (CIE) coordinate of (0.16, 0.16). Furthermore, the device demonstrated the excellent performances with a maximum current efficiency (CE) of 10.5 cd A^{-1}, a maximum power efficiency (PE) of 5.5 lm W^{-1}, and a maximum EQE of 7.8% (at 84 cd m^{-2}, **Figure 4**), which is among the best results in nondoped blue emissive OLED that have ever been reported as far as we know.[16] A distinct virtue is that the device exhibited robust stability; the device still maintained an outstanding performance with CE of 4.2 cd A^{-1}, PE of 2.5 lm W^{-1}, and EQE of 5.6% under the brightness of 1000 cd m^{-2}.

Furthermore, the maximum η_s of EL devices can be estimated according to Equation (2)

$$\eta_s = \eta_{rec} \times \eta_{PL} \times \eta_{out} \div \eta_{EL} \quad (2)$$

where η_{out} (≈$1/2n^2$) is the light out-coupling efficiency (for glass substrates, n = 1.5, η_{out} is estimated as ≈20%); η_{rec} is the efficiency for electron–hole recombination, which could be assumed as 100% in a properly designed EL device; η_{PL} of TBPMCN is ≈40% as mentioned above.[15] Notably, the η_s of TBPMCN is calculated to be 97%, which is almost a full exciton utilization, and is far superior to the 25% spin statistics limit. Compared with η_s (85%) in TPMCN, slightly increased η_s is harvested in TBPMCN due to the maintained CT component from the similar cyano substitution.

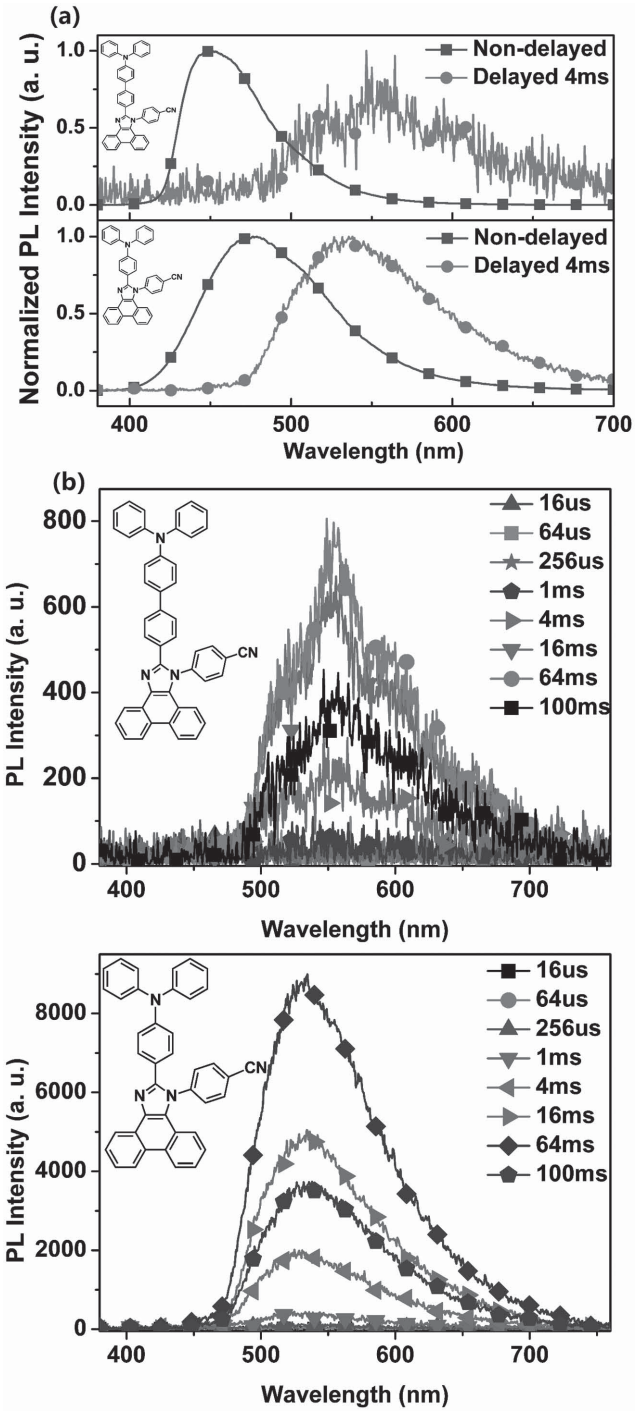

Figure 3. Time-resolved PL spectra of TPMCN and TBPMCN at 77 K, measured on a LP-920. The concentration of the solutions are 5×10^{-6} mol L^{-1}. a) The nondelayed fluorescent spectra and the 4 ms-delayed phosphorescent spectra. b) Phosphorescent spectra of different delayed time scales.

To clarify the nature of high η_s, some further analysis and measurement are necessary for TBPMCN. First, the high η_s in TBPMCN should not be ascribed to the TTA mechanism,[17] because in that case, the η_s should not exceed its upper limit of 62.5%,[14] and the current-density–brightness curve of TBPMCN

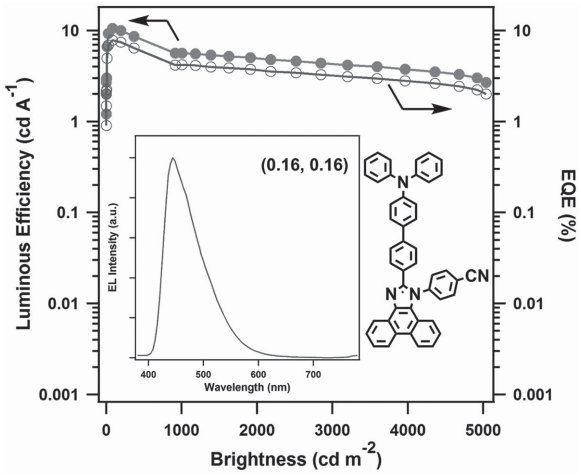

Figure 4. Nondoped EL performance of TBPMCN. The EL device structure is ITO/PEDOT:PSS (40 nm)/NPB (80 nm)/TCTA (5 nm)/TBPMCN (20 nm)/TPBi (40 nm)/LiF (1 nm)/Al (120 nm).

is in strong linearity without the deviation of luminance saturation in EL device (Figure S10, Supporting Information). We then performed transient EL measurement on TBPMCN with a typical TADF material 4CZTPN-PH as the reference to identify the different EL mechanisms between them,[6a] in order to see if there is any delayed component in the EL of TBPMCN. As shown in **Figure 5**, the transient pulse voltage width is set as 20 μs within the whole measurement period of 200 μs. In a very short time range after this transient pulse (about 20–20.5 μs),[7b,19] the EL is dominated by the radiative decay of the radiative excitons generated before the voltage is off in the EL device. Obviously, the TADF material 4CZTPN-PH shows very flat EL decay curve, which should be attributed to the time-consuming TADF process for the exciton conversion from triplet to singlet. As a comparison, TBPMCN demonstrates very sharp EL decay curve in the same time range, indicating that almost all of the radiative excitons in TBPMCN are short-lived

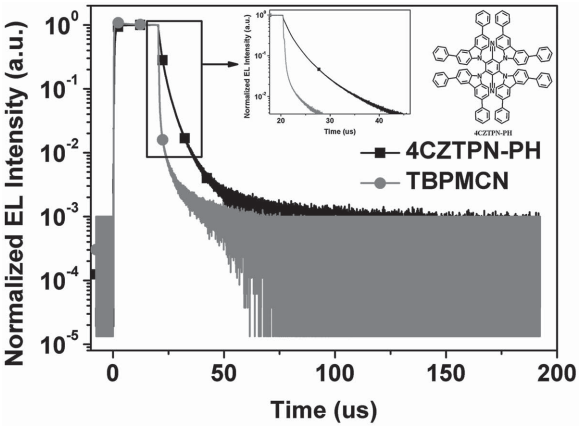

Figure 5. Transient EL measurement for 4CZTPN-PH and TBPMCN. The EL device structures are constructed as ITO/4, 4-bis[N-(1-naphthyl)-N-phenylamino]-biphenyl (α-NPD, 35 nm)/4CZTPN-PH:4, 4–9-bis (carbazol-9-yl)-biphenyl (CBP) (5 ± 1 wt %) (15 nm)/TPBI (65 nm)/LiF (0.8 nm)/Al (70 nm) for 4CZTPN-PH and ITO/α-NPD (30 nm)/TBPMCN (20 nm)/TPBi (40 nm)/LiF (1 nm)/Al (120 nm) for TBPMCN.

component without TADF contribution. In a whole, the high η_s in TBPMCN suit neither TTA nor TADF mechanisms.

As for a possible mechanism, tentatively, we propose that the triplet excitons can be converted into the singlet excitons in TBPMCN through a ultrafast RISC process along a high-lying excited state, namely, the "hot" CT channels.[6d,7] As a matter of fact, the "hot" CT channels are beneficial to the effective triplet exciton conversion in EL process without any delayed fluorescence. In EL process, the intermolecular CT excitons are initially generated with very weak binding energy on the higher excited states, and the triplet exciton can be more easily converted into the singlet one along the "hot" CT channel.[20] As a result, a near 100% exciton utilization can be harvested in TBPMCN-like phosphorescent materials and TADF materials. Ultimately, the quasi-equivalently hybridized material TBPMCN exhibits much better device performances than nonequivalently hybridized TPMCN, as a result of fine modulation in excited states: near threefold η_{PL} (from 13% to 40%) and a slightly improved η_s (from 85% to 97%) are achieved, due to the enhanced LE component in the presence of an extra middle phenyl ring and more sufficient hybridization between LE and CT components according to the theoretical calculations. In other words, the coexisting LE and CT characters in TBPMCN could ensure not only high η_{PL} but also high η_s in EL device, and their golden combination causes the best efficiency of OLEDs.

3. Conclusion

In summary, we reported a highly efficient pure blue electrofluorescent material TBPMCN, harvesting a nearly fourfold EL efficiency upon the insertion of only one phenyl ring. Based on the CT-dominated material TPMCN, a fine modulation on emissive state was performed between LE and CT components to form a quasi-equivalent hybridized HLCT state in TBPMCN. The LE component contributes a high η_{PL}, while the CT component facilitates a high η_s derived from the enhanced RISC (T→S). It is confirmed by theoretical calculations and photophysical experiment that for TBPMCN, more sufficient hybridization of LE and CT components are in its excited states, and this golden combination of LE and CT finally leaded to the dramatically enhanced EL performance as a maximum current efficiency of 10.5 cd A^{-1}, a maximum EQE of 7.8%, and a nearly 100% exciton utilization in nondoped EL device. This approach would be an ideal strategy to design the next-generation high-efficiency, low-cost organic EL materials with simultaneous high PL efficiency and high exciton utilization in nondoped OLEDs by a golden combination between LE and CT components.

4. Experimental Section

General Methods: All of the reagents and solvents used for synthesis were purchased from Aldrich or Acros and used as received. All of the reactions were performed under a nitrogen atmosphere. The ^{1}H-nuclear magnetic resonance (NMR) and ^{13}C-NMR spectra were recorded on an AVANCZ 500 spectrometers at 298 K by utilizing deuterated dimethyl sulfoxide (DMSO) as solvents and tetramethylsilane (TMS) as a standard. The elemental analysis was implemented on a Flash EA 1112, CHNS-O elemental analysis instrument. The matrix-assisted laser desorption/ionization time of flight mass spectrometry (MALDI-TOF-MS) were recorded using an AXIMA-CFRTM plus instrument. The UV–vis absorption spectra were recorded on a UV-3100 spectrophotometer. The fluorescent spectra were carried out with a RF-5301PC. The room-temperature lifetimes were measured on an Edinburgh FLS-980 with an EPL-375 optical laser. The film PL efficiencies were measured on a Gliden Fluorescence System. The time-resolved PL spectra were measured on an Edingburg LP-920. The temperature-dependent spectra and lifetimes were measured on an Edingburg FLS-920. For the transient EL experiments, we used an Agilent 8114A pulse generator (100 V/2 A) to generate rectangular pulse voltages to our devices. The pulse repetition rate was 1 kHz with the width of 200 μs. The emission was collected by a lens coupled with the optical fiber connected to a Hamamatsu photomultiplier (H10721-20) with time resolution of 0.57 ns. The photomultiplier was connected to one of the channel of a digital oscilloscope (Tektronix DPO7104, sampling rate: 5 GS s^{-1}; resolution: 100 μV) with 50 Ω input resistance.

Synthesis of 4-(2-(4-Bromophenyl)-1H-Phenanthro[9,10-d]Imidazol-1-yl)Benzonitrile (BrBPMCN):[18] A mixture of 5.0 mmol (920 mg) 4-bromobenzaldehyde, 5.0 mmol (1.04 g) phenanthrenequinone, 20 mmol (2.36 mg) 4-aminobenzonitrile, and 25 mmol (1.85 g) ammonium acetate with 15 mL acetic acid were added into a clean 100 mL flask and refluxed under N_2 in a 120 °C oil bath for 2 h. After cooling down, the solid product was filtrated and washed with 30 mL 1:1 water/acetic acid and 30 mL water successively, dissolved in $CHCl_3$ and dried in $MgSO_4$ overnight, purified by thin layer chromatography and 2.08 g (4.4 mmol) white product was obtained, yield 88%: MS: 474.6 ($M(H^+)$), ^{1}H NMR (500 MHz, DMSO) δ = 8.96 (d, J = 8.2, 1H), 8.90 (d, J = 8.3, 1H), 8.69 (d, J = 7.2, 1H), 8.20 (d, J = 8.3, 2H), 8.01 (d, J = 8.4, 2H), 7.79 (t, J = 7.5, 1H), 7.72 (t, J = 7.2, 1H), 7.61 (t, J = 9.3, 3H), 7.47 (d, J = 8.5, 2H), 7.42 (t, J = 7.7, 1H), 7.07 (d, J = 8.2, 1H). The product was directly used as the reactant of the next step without further purification.

Synthesis of TBPMCN: A mixture of 2.0 mmol (912 mg) BrBPMCN, 2.0 mmol (740 mg) *N*,*N*-diphenyl-4-(4,4,5,5-tetramethyl-1,3,2-dioxaborolan-2-yl)aniline, 20 mmol (2.16 g) potassium carbonate, and 60 mg (0.052 mmol) tetrakis-(triphenylphosphine)-palladium(0) ($Pd(PPh_3)_4$) with 8 mL deionized water and 10 mL toluene were added into a clean 50 mL flask and refluxed for two days under N_2 atmosphere. The organic phase was washed with 20 mL water and extracted with $CHCl_3$, then was dried in $MgSO_4$ overnight and purified by thin layer chromatography. Finally, 700 mg (1.1 mmol) pure dry white product was obtained, yield 55%: MS: 639.8 ($M(H^+)$), ^{1}H-NMR (500 MHz, DMSO) δ = 8.97 (d, J = 8.5, 1H), 8.91 (d, J = 8.7, 1H), 8.71 (d, J = 7.5, 1H), 8.22 (d, J = 8.4, 2H), 8.05 (d, J = 8.5, 2H), 7.80 (d, J = 7.0, 1H), 7.74–7.63 (m, 5H), 7.59 (d, J = 8.0, 3H), 7.42 (s, 1H), 7.35 (t, J = 7.9, 4H), 7.09 (dd, J = 14.3, 7.4, 7H), 7.04 (d, J = 8.7, 2H), ^{13}C-NMR (126 MHz, $CDCl_3$), δ = 150.55, 147.83, 147.51, 142.70, 141.48, 134.03, 133.38, 130.29, 129.90, 129.42, 128.42, 127.63, 126.60, 126.60–125.80, 125.35, 124.64, 124.54, 123.60, 123.35–122.65, 122.39, 120.49, 117.68, 113.95. Elemental analysis: calculated for $C_{46}H_{30}N_4$: C, 86.49; H, 4.73; N, 8.77; found: C, 86.66; H, 4.59; N, 8.72.

Supporting Information

Supporting Information is available from the Wiley Online Library or from the author.

Acknowledgements

The authors thank Dr. Veaceslav Coropceanu, Georgia Institute of Technology, Atlanta, USA, for the fruitful discussion. This work is supported by the National Natural Science Foundation of China (51273078, 91233113, 51203091, and 51473063), the Ministry of Science and Technology of China (2013CB834801, 2015CB655003),

and the Graduate Innovation Fund of Jilin University (Project No. 2014011).

Received: December 2, 2014
Revised: January 23, 2015
Published online: February 11, 2015

[1] C. W. Tang, S. A. VanSlyke, *Appl. Phys. Lett.* **1987**, *51*, 913.
[2] a) Y. G. Ma, H. Y. Zhang, J. C. Shen, C. M. Chen, *Synth. Met.* **1998**, *94*, 245; b) M. A. Baldo, D. F. O'brien, Y. You, A. Shoustikov, S. Sibley, M. E. Thompson, S. R. Forrest, *Nature* **1998**, *395*, 151.
[3] a) M. A. Baldo, S. Lamansky, P. E. Burrows, M. E. Thompson, S. R. Forrest, *Appl. Phys. Lett.* **1999**, *75*, 4; b) Y. Cao, I. D. Parker, G. Yu, C. Zhang, A. J. Heeger, *Nature* **1999**, *397*, 414; c) Z. Shuai, D. Beljonne, R. J. Silbey, J. L. Brédas, *Phys. Rev. Lett.* **2000**, *84*, 131.
[4] C. Adachi, M. A. Baldo, M. E. Thompson, S. R. Forrest, *J. Appl. Phys.* **2001**, *90*, 5048.
[5] C. J. Chiang, A. Kimyonok, M. K. Etherington, G. C. Griffiths, V. Jankus, F. Turksoy, A. P. Monkman, *Adv. Funct. Mater.* **2013**, *23*, 739.
[6] a) H. Uoyama, K. Goushi, K. Shizu, H. Nomura, C. Adachi, *Nature* **2012**, *492*, 234; b) Q. Zhang, B. Li, S. Huang, H. Nomura, H. Tanaka, C. Adachi, *Nat. Photonics* **2014**, *8*, 326; c) H. Tanaka, K. Shizu, H. Miyazaki, C. Adachi, *Chem. Commun.* **2012**, *48*, 11392; d) Q. Zhang, J. Li, K. Shizu, S. Huang, S. Hirata, H. Miyazaki, C. Adachi, *J. Am. Chem. Soc.* **2012**, *134*, 14706.
[7] a) W. J. Li, D. D. Liu, F. Z. Shen, D. G. Ma, Z. M. Wang, T. Fei, B. Yang, Y. G. Ma, *Adv. Funct. Mater.* **2012**, *22*, 2797; b) W. J. Li, Y. Y. Pan, R. Xiao, Q. M. Peng, S. T. Zhang, D. G. Ma, F. Li, F. Z. Shen, Y. H. Wang, B. Yang, Y. G. Ma, *Adv. Funct. Mater.* **2014**, *24*, 1609; c) S. Tang, W. J. Li, F. Z. Shen, D. D. Liu, B. Yang, Y. G. Ma, *J. Mater. Chem.* **2012**, *22*, 4401; d) S. T. Zhang, W. J. Li, L. Yao, Y. Y. Pan, B. Yang, Y. G. Ma, *Chem. Commun.* **2013**, *49*, 11302; e) L. Yao, S. T. Zhang, R. Wang, W. J. Li, F. Z. Shen, B. Yang, Y. G. Ma, *Angew. Chem. Int. Ed.* **2014**, *53*, 2119; f) B. Yang, Y. G. Ma, *Sci. China Ser. B* **2013**, *43*, 1457; g) Y. Y. Pan, W. J. Li, S. T. Zhang, L. Yao, C. Gu, H. Xu, B. Yang, Y. G. Ma, *Adv. Opt. Mater.* **2014**, *2*, 510; h) W. J. Li, Y. Y. Pan, L. Yao, H. C. Liu, S. T. Zhang, C. Wang, F. Z. Shen, B. Yang, Y. G. Ma, *Adv. Opt. Mater.* **2014**, *2*, 892.
[8] a) D. Chaudhuri, E. Sigmund, A. Meyer, L. Rçck, P. Klemm, S. Lautenschlager, A. Schmid, S. R. Yost, T. Van Voorhis, S. Bange, S. Hçger, J. M. Lupton, *Angew. Chem.* **2013**, *125*, 13691; b) D. Chaudhuri, E. Sigmund, A. Meyer, L. Rçck, P. Klemm, S. Lautenschlager, A. Schmid, S. R. Yost, T. Van Voorhis, S. Bange, S. Hçger, J. M. Lupton, *Angew. Chem. Int. Ed.* **2013**, *52*, 13449.
[9] a) M. J. Frisch, G. W. Trucks, H. B. Schlegel, G. E. Scuseria, M. A. Robb, J. R. Cheeseman, G. Scalmani, V. Barone, B. Mennucci, G. A. Petersson, H. Nakatsuji, M. Caricato, X. Li, H. P. Hratchian, A. F. Izmaylov, J. Bloino, G. Zheng, J. L. Sonnenberg, M. Hada, M. Ehara, K. Toyota, R. Fukuda, J. Hasegawa, M. Ishida, T. Nakajima, Y. Honda, O. Kitao, H. Nakai, T. Vreven, J. A. Montgomery Jr., J. E. Peralta, F. Ogliaro, M. Bearpark, J. J. Heyd, E. Brothers, K. N. Kudin, V. N. Staroverov, R. Kobayashi, J. Normand, K. Raghavachari, A. Rendell, J. C. Burant, S. S. Iyengar, J. Tomasi, M. Cossi, N. Rega, J. M. Millam, M. Klene, J. E. Knox, J. B. Cross, V. Bakken, C. Adamo, J. Jaramillo, R. Gomperts, R. E. Stratmann, O. Yazyev, A. J. Austin, R. Cammi, C. Pomelli, J. W. Ochterski, R. L. Martin, K. Morokuma, V. G. Zakrzewski, G. A. Voth, P. Salvador, J. J. Dannenberg, S. Dapprich, A. D. Daniels, O. Farkas, J. B. Foresman, J. V. Ortiz, J. Cioslowski, D. J. Fox, *Gaussian 09, Revision B.01*, Gaussian, Inc., Wallingford, CT **2009**; b) R. L. Martin, *J. Chem. Phys.* **2003**, *118*, 4775.
[10] a) S. P. Jagtap, S. Mukhopadhyay, V. Coropceanu, G. L. Brizius, J. Brédas, D. M. Collard, *J. Am. Chem. Soc.* **2012**, *134*, 7176; b) S. Shirai, S. Iwata, T. Tani, S. Inagaki, *J. Phys. Chem. A* **2011**, *115*, 7687.
[11] Z. R. Grabowski, K. Rotkiewicz, W. Rettig, *Chem. Rev.* **2003**, *103*, 3899.
[12] E. Lippert, W. Lüder, H. Boos, *Advances in Molecular Spectroscopy*, (Ed: A. Mangini) Pergamon, Oxford **1962**.
[13] J. Birks, *Photophysics of Aromatics Molecules*, Wiley, New York **1970**.
[14] S. Sinha, C. Rothe, R. Güntner, U. Scherf, A. P. Monkman, *Phys. Rev. Lett.* **2003**, *90*, 127402.
[15] J. R. Sheats, H. Antoniadis, M. Hueschen, W. Leonard, J. Miller, R. Moon, D. Roitman, A. Stocking, *Science* **1996**, *273*, 884.
[16] a) M. R. Zhu, C. L. Yang, *Chem. Soc. Rev.* **2013**, *42*, 4963; b) H. H. Chou, Y. H. Chen, H. P. Hsu, W. H. Chang, Y. H. Chen, C. H. Cheng, *Adv. Mater.* **2012**, *24*, 5867; c) R. Kim, S. Lee, K. H. Kim, Y. J. Lee, S. K. Kwon, J. J. Kim, Y. H. Kim, *Chem. Commun.* **2013**, *49*, 4664; d) C. G. Zhen, Z. K. Chen, Q. D. Liu, Y. F. Dai, R. Y. C. Shin, S. Y. Chang, J. Kiffer, *Adv. Mater.* **2009**, *21*, 2425; e) C. G. Zhen, Y. F. Dai, W. J. Zeng, Z. Ma, Z. K. Chen, J. Kiffer, *Adv. Funct. Mater.* **2011**, *21*, 699; f) Y. Zou, J. H. Zou, T. L. Ye, H. Li, C. L. Yang, H. B. Wu, D. G. Ma, J. G. Qin, Y. Cao, *Adv. Funct. Mater.* **2013**, *23*, 1781; g) J. Y. Hu, Y. J. Pu, F. Satoh, S. Kawata, H. Katagiri, H. Sasabe, J. Kido, *Adv. Funct. Mater.* **2013**, *24*, 2604; h) C. Liu, Q. Fu, Y. Zou, C. L. Yang, D. G. Ma, J. G. Qin, *Chem. Mater.* **2014**, *26*, 3074; i)Z. Gao, G. Cheng, F. Z. Shen, S. T. Zhang,Y. N. Zhang,P. Lu, Y. G. Ma, *Laser Photonics Rev.* **2014**, *8*, L6; j)Z. Gao, Z. M. Wang,T. Shan,Y. L. Liu,F. Z. Shen,Y. Y. Pan, H. H. Zhang,X. He,P. Lu,B. Yang,Y. G. Ma, *Org. Electron.* **2015**, *15*, 2667; k)Z. Gao, Y. L. Liu, Z. M. Wang,F. Z. Shen,H. Liu, G. N. Sun, L. Yao, Y. Lv, P. Lu, Y. G. Ma, *Chem. Eur. J.* **2013**, *19*, 2602.
[17] T. Nakagawa, S. Y. Ku, K. T. Wong, C. Adachi, *Chem. Commun.* **2012**, *48*, 9580.
[18] Z. M. Wang, P. Lu, S. M. Chen, Z. Gao, F. Z. Shen, W. S. Zhang, Y. X. Xu, H. S. Kwok, Y. G. Ma, *J. Mater. Chem.* **2011**, *21*, 5451.
[19] W. Barford, R. J. Bursill, D. V. Marhov, *Phys. Rev. B* **2010**, *81*, 035206.
[20] a) M. Segal, M. Singh, K. Rivoir, S. Difley, T. V. Voorhis, M. A. Baldo, *Nat. Mater.* **2007**, *6*, 374; b) S. Difley, D. Beljonne, T. V. Voorhis, *J. Am. Chem. Soc.* **2008**, *13*, 3420; c) W. Barford, *Phys. Rev. B* **2004**, *70*, 205204.